

# Inhibition of Quorum Sensing and Biofilm Formation in *Chromobacterium violaceum* by Fruit Extracts of *Passiflora edulis*

Mahendrarajan Venkatramanan,<sup>♦</sup> Pitchaipillai Sankar Ganesh,<sup>♦</sup> Renganathan Senthil,  
Jeyachandran Akshay, Arumugam Veera Ravi, Kulanthaivel Langeswaran, Jamuna Vadivelu,\*  
Samuthira Nagarajan, Kaliaperumal Rajendran, and Esaki Muthu Shankar\*



Cite This: *ACS Omega* 2020, 5, 25605–25616



Read Online

ACCESS |



Metrics & More

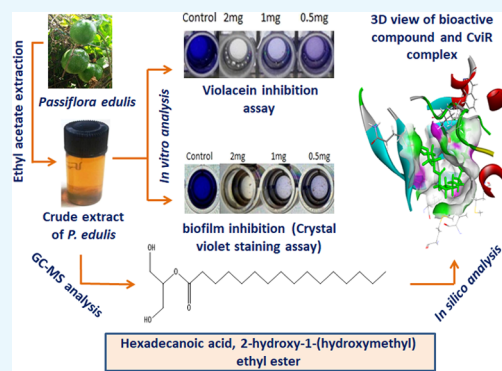


Article Recommendations



Supporting Information

**ABSTRACT:** *Chromobacterium violaceum* (*C. violaceum*) is a Gram-negative, rod-shaped facultatively anaerobic bacterium implicated with recalcitrant human infections. Here, we evaluated the anti-QS and antibiofilm activities of ethyl acetate extracts of *Passiflora edulis* (*P. edulis*) on the likely inactivation of acyl-homoserine lactone (AHL)-regulated molecules in *C. violaceum* both by in vitro and in silico analyses. Our investigations showed that the sub-MIC levels were 2, 1, and 0.5 mg/mL, and the concentrations showed a marked reduction in violacein pigment production by 75.8, 64.6, and 35.2%. AHL quantification showed 72.5, 52.2, and 35.9% inhibitions, inhibitions of EPS production (72.8, 36.5, and 25.9%), and reductions in biofilm formation (90.7, 69.4, and 51.8%) as compared to a control. Light microscopy and CLSM analysis revealed dramatic reduction in the treated biofilm group as compared to the control. GC–MS analysis showed 20 major peaks whose chemical structures were docked as the CviR ligand. The highest docking score was observed for hexadecanoic acid, 2-hydroxy-1-(hydroxymethyl) ethyl ester bonds in the active site of CviR with a binding energy of  $-8.825$  kcal/mol. Together, we found that hexadecanoic acid, 2-hydroxy-1-(hydroxymethyl) ethyl ester remarkably interacted with CviR to inhibit the QS system. Hence, we concluded that hexadecanoic acid, 2-hydroxy-1-(hydroxymethyl) ethyl ester of *P. edulis* could likely be evaluated for treating *C. violaceum* infections.



## 1. INTRODUCTION

*Chromobacterium violaceum* (*C. violaceum*) is a large, motile, free-living, and saprophytic Gram-negative bacterium that inhabits fresh-water and soil environments, and it is cosmopolitan in distribution.<sup>1</sup> Although rare, *C. violaceum* is implicated with a highly fatal septicemia in human subjects.<sup>2</sup> Furthermore, it has also been reported to be causes of certain orphan infections such as necrotizing metastatic abscesses involving the lungs, liver, spleen, brain, and lymph nodes.<sup>3,4</sup> Accumulating lines of evidence also indicate its role in pneumonia,<sup>5</sup> urinary tract infections,<sup>6</sup> meningitis,<sup>7</sup> endocarditis, and bacteria-associated hemophagocytic syndrome.<sup>8</sup> *C. violaceum* is resistant to a broad spectrum of antibiotics, especially beta-lactams like penicillin, ampicillin, and cephalosporins.<sup>9</sup>

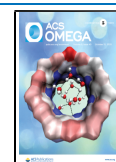
Regarding the various virulence attributes present in Gram-negative bacteria, the most important represents a quorum sensing (QS) system that protects the bacterial species from antibiotic/drug pressure and helps the bacterium to form the biofilm in tissues resulting in diagnostic predicaments and treatment difficulties.<sup>10</sup> QS refers to a mechanism that involves cell-to-cell communication in which bacteria cross-talk with each other via small signaling molecules called autoinducers

(AIs). The QS system of *C. violaceum* consists of two components such as CviI and CviR (LuxI/LuxR homologue) genes producing and responding with a high affinity to acyl-homoserine lactone (AHL) molecules. Evidence indicates that the CviI AHL synthase mediates the synthesis of *N*-decanoyl-L-homoserine lactone (C10-HSL), a signaling molecule, and CviR, a transcriptional regulatory protein.<sup>11,12</sup> With the eventual increase in bacterial cell population, the AHL molecules bind to their cognate receptors to form a complex that regulates the expression of target genes (including the *vioABCDE* operon), which engenders the production of a purple violacein pigment and formation of biofilm matrices in *C. violaceum*.<sup>13</sup> Similarly, the QS system controls the secretion of virulence factors such as metalloproteases, type II (TISS) and type III (TISS) secretion systems, swarming motility, exopolysaccharide (EPS), lipases, flagellar proteins, collagen-

Received: May 27, 2020

Accepted: August 12, 2020

Published: September 29, 2020



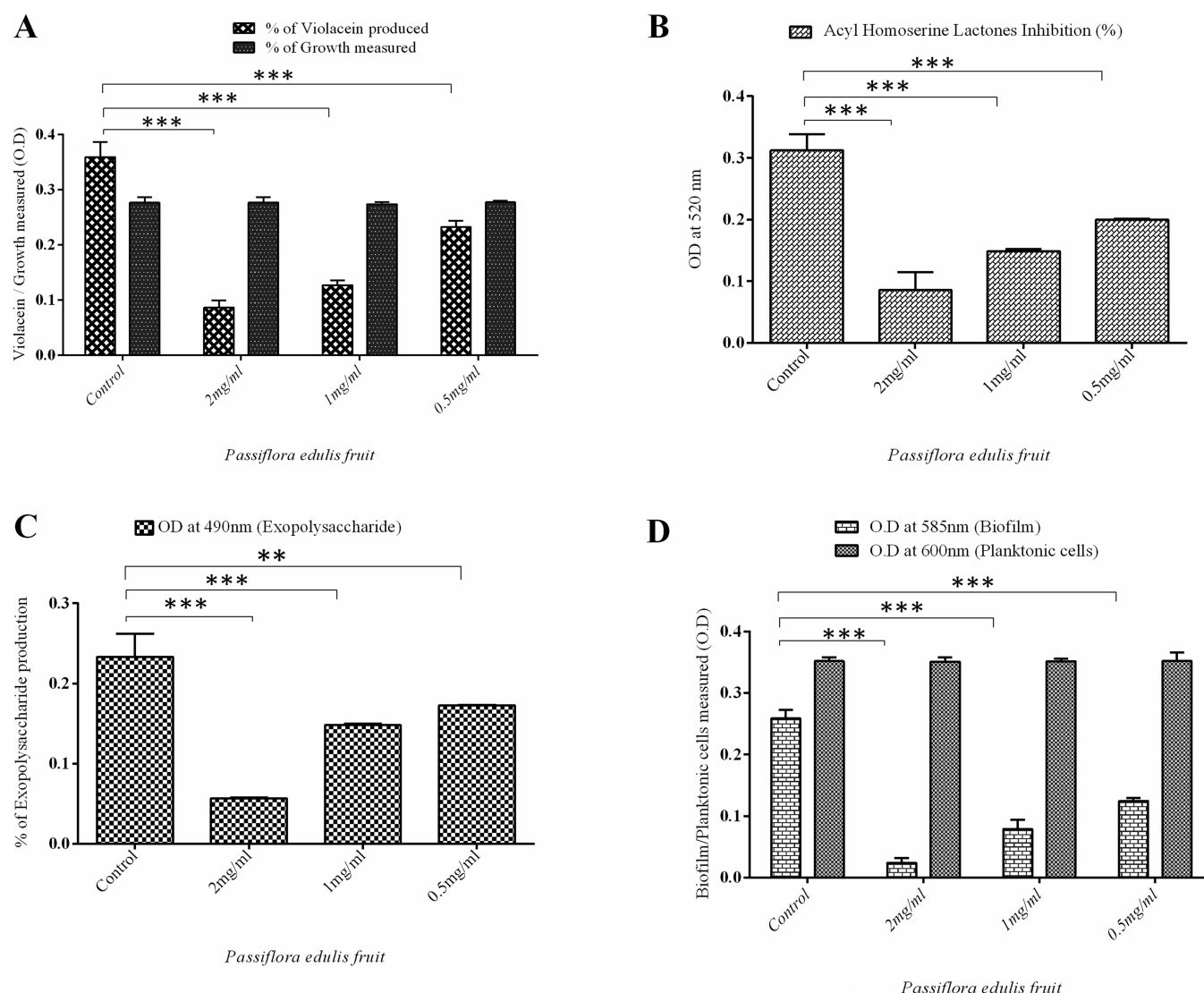


**Figure 1.** Effect of sub-inhibitory concentrations of EA extract of *P. edulis* (2, 1, and 0.5 mg/mL) on QS-mediated virulence factors and biofilm formation in *C. violaceum*: (A) quantification of violacein produced in percentage with respect to a control (untreated), more than 75.8% (2 mg/mL) inhibition of violacein production was observed at 2 mg/mL and measured bacterial growth OD at 600 nm; (B) the quantitative assessment of AHL inhibition of *C. violaceum* by EA extract of *P. edulis* at the concentrations of 2, 1, and 0.5 mg/mL; (C) effect of EA extract of *P. edulis* on EPS production by *C. violaceum*: the EA extract inhibited EPS production by *C. violaceum* at 2, 1, and 0.5 mg/mL (72.8, 36.5, and 25.9%); (D) inhibition of biofilm formation in *C. violaceum* treated with EA extract of *P. edulis* (2, 1, and 0.5 mg/mL) and measured the planktonic cell growth at 600 nm ( $p < 0.01$  and  $p < 0.001$ ).

nase, chitinase, and cytolytic toxins.<sup>14–16</sup> The secretion of the aforementioned extracellular virulence factors together with biofilm formation are implicated with the establishment of infection in host cells and the development of resistance to several antimicrobial agents.<sup>17–20</sup>

A wide array of QS systems operate across pathogenic bacterial species, for instance in Gram-negative bacteria such as *Burkholderia pseudomallei*, *Stenotrophomonas maltophilia*, *Escherichia coli*, *Vibrio cholerae*, *Acinetobacter baumannii*, *Pseudomonas aeruginosa*, and *Burkholderia cepacia*<sup>21</sup> as well as in certain plant pathogens like *Erwinia carotovora* and *Ralstonia solanacearum* that are studied extensively for their QS-controlled virulence and pathogenicity attributes.<sup>22,23</sup> Given the established involvement of a QS system in the regulation of virulence factors and biofilms in *C. violaceum*, interventions aimed at targeting such a system likely contributes to the

development of promising therapeutic strategies against recalcitrant infections.

The natural ecosystem offers a rich repertoire of biologically and chemically diverse bioactive compounds. Edible fruits and secondary metabolites are a rich source of antioxidants and are also known for their anti-inflammatory, immunomodulatory, and antimicrobial potentials.<sup>24</sup> Nonetheless, only a limited number of anti-QS and antibiofilm analogues have thus far been identified in edible fruits. The Indian system of culinary, plants, shrubs, and fruits (turmeric, garlic, pea and soybean) indigenous to the subcontinent represents a rich source of QS inhibitors, and a few have already been reported to inhibit AHL-dependent QS reporters in *C. violaceum*.<sup>25</sup> For instance, furocoumarins and limonoids of the grape vine have shown strong anti-QS (AI-1 and AI-2) and antibiofilm potentials in *Vibrio harveyi* and *E. coli*.<sup>26,27</sup> Similarly, extracts of edible fruits such as *Ananas comosus*, *Musa paradisiaca*, *Manilkara zapota*,

and *Ocimum sanctum* have previously been shown to inactivate AHL molecules produced by *C. violaceum* and *P. aeruginosa*, albeit at defined concentrations.<sup>28</sup>

*Passiflora edulis* (passion fruit, *P. edulis*) is an edible fruit used widely in the Indian culinary and food industry. *P. edulis* is also cultivated widely across the tropical and subtropical regions of the world.<sup>29</sup> The fruit is a rich source of certain phytochemicals, especially harman, harmalin, vitexin, carotenoids, passafiorine, and theobromine. The plant leaves and flowers are also used to treat arthritis, diabetes, hypertension, inflammatory conditions, asthma, insomnia, menopausal symptoms, convulsions, central nervous system manifestations, anxiety, and gastrointestinal disorders. *P. edulis* (seeds) has been shown to possess antioxidant, antibacterial, and antifungal properties.<sup>30</sup> However, the compound(s) responsible for the anti-QS and antibiofilm activities present in *P. edulis* (fruit) largely remain(s) ambiguous. Therefore, we aimed to evaluate the anti-QS and antibiofilm activities for likely inactivation of AHL-regulated molecules in *C. violaceum* both by in vitro and in silico analyses.

## 2. RESULTS

**2.1. Effects of EA Extracts of *P. edulis* on QS-Mediated Virulence Factors in *C. violaceum*.** The crude extracts of *P. edulis* using two organic solvents, methanol and ethyl acetate, were employed to optimize the anti-QS and antibiofilm activities on a control strain of *C. violaceum* (CV12472). The methanol and EA extracts inhibited the growth of *C. violaceum* at a concentration of 5 mg/mL. Further, the methanol and EA extracts of *P. edulis* were screened for anti-QS activities. Although the methanol extract failed to inhibit violacein production at the sub-MIC concentration (data not shown), the EA extract of *P. edulis* showed promising anti-QS activity at the sub-MIC level in a dose-dependent manner. The EA extract inhibited violacein pigments (75.8, 64.6, and 35.2%) at the sub-MIC concentrations of 2, 1, and 0.5 mg/mL. The percentage inhibition of the violacein pigment by the EA extract of *P. edulis* is shown in Figure 1A. At the tested sub-MIC concentrations, the EA extract did not show any growth inhibition, but remarkably, it inhibited violacein pigment production in a dose-dependent manner. By quantitative determination, the EA extract was found to inhibit the production of AHLs at 72.5, 52.2, and 35.9%, in contrast to the control (without EA extract), in the presence of 2, 1, and 0.5 mg/mL, respectively (Figure 1B). Together, our results indicated that the EA extract remarkably inhibited AHL production relative to the control.

Flagella-mediated swarming motility plays a pivotal role in QS-controlled biofilm formation in *C. violaceum*. In the present study, the EA extract of *P. edulis* significantly reduced swarming motility at the concentrations of 2, 1, and 0.5 mg in comparison to the untreated control (Figure 2A–D). The study also demonstrated that the EA extract of *P. edulis* at 2, 1, and 0.5 mg/mL concentrations inhibited EPS production in *C. violaceum* (CV12472) at the levels of 72.8, 36.5, and 25.9%, respectively (Figure 1C), indicating that *P. edulis* alleviated EPS production in *C. violaceum* and affected the architecture of the biofilm.

**2.2. Effect of EA Extracts of *P. edulis* on Biofilm Formation in *C. violaceum*.** The EA extract inhibited *C. violaceum* (CV12472) biofilm formation in a dose-dependent manner (Figure 1D). The EA extract of *P. edulis* showed significant reduction in biofilm formation when the organisms

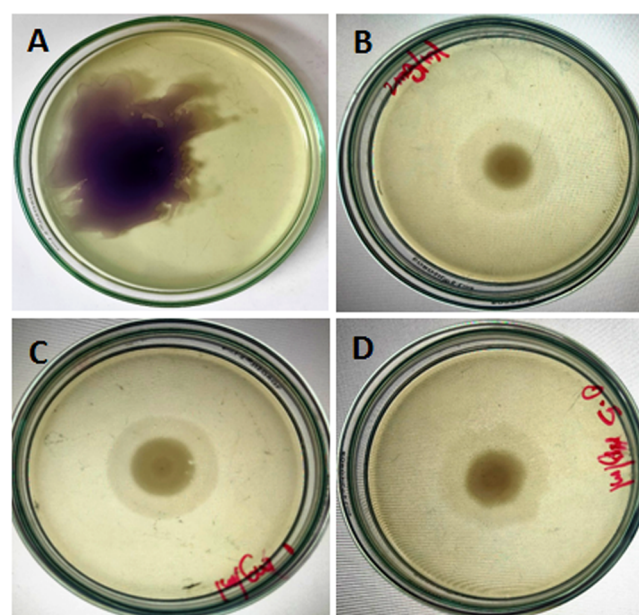


**Figure 2.** Inhibitory effect of EA extract of *P. edulis* on the swarming motility of *C. violaceum* (CV12472). (A) Control (without EA extract). (B) The bacterial cells were inoculated at the center of the agar medium containing EA extract of *P. edulis* at the concentration of 2 mg/mL, (C) 1 mg/mL, and (D) 0.5 mg/mL, and the plates were incubated at 30 °C for 24 h.

were grown in the presence of 2 mg/mL (90.7%), 1 mg/mL (69.4%), and 0.5 mg/mL (51.8%), respectively, relative to the control (i.e., without EA extract). Similarly, when the effect of planktonic cell growth was quantified, there was no significant variation at the 600 nm value of planktonic cell suspension suggesting that the EA extract did not have any added impact on the planktonic cell growth in *C. violaceum* (CV12472) (Figure 1D).

When the effect of the EA extract on biofilm formation was analyzed using light microscopy, we observed bacterial aggregation (biofilm matrix) on the surface of the cover slip in the control (without treatment) group. We also observed a drastic reduction in the biofilm cluster in the EA extract-treated *C. violaceum* (CV12472) as compared to that of the control (Figure 3A–D).

Next, we studied the three-dimensional architectural complexity of the *C. violaceum* (CV12472) biofilm both in the presence and absence of the EA extract of *P. edulis* using CLSM. We observed a marked reduction in biofilm thickness, and biomass was observed in the EA extract-treated biofilm on the surface of the cover slip (Figure 3E–H). The inhibitory effects of 2, 1, and 0.5 mg/mL EA extracts were confirmed by the CLSM image of the *C. violaceum* (CV12472) biofilm (Figure 3E–H).

**2.3. Identification of Chemical Constituents by GC–MS.** Next, the chemical constituents of the EA extract of *P. edulis* were identified by GC–MS, and the mass spectra of chemical constituents of active compounds were identified by searching in NIST and Wiley libraries. Subsequently, we identified and characterized a total of 20 chemical constituents (Table 1). The total ion chromatogram (TIC) of *P. edulis* confirmed the presence of various biologically active compounds with different retention times (RTs) (Figure 4). The mass spectrometric (MS) analysis of the chemical constituents eluted at different time intervals helped to identify



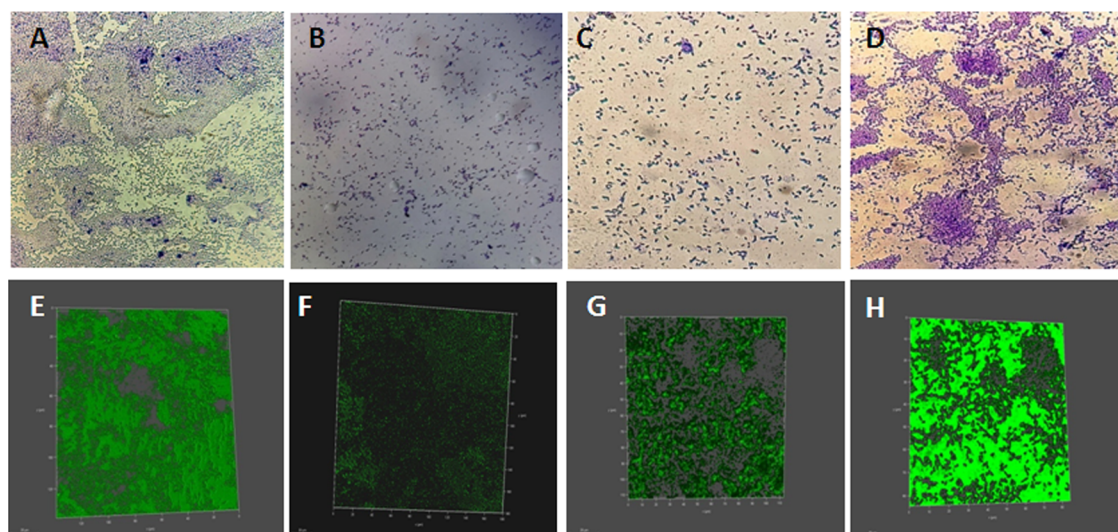


**Figure 3.** In situ light microscopy and confocal laser scanning microscope analysis of antibiofilm activities of *P. edulis* (EA extract) in *C. violaceum*: light microscopy analysis of biofilm formation in *C. violaceum* (CV12472): (A) Control shows biofilm formation after 24 h of incubation, (B) the EA extract of *P. edulis* reduced the biofilm matrix at a concentration of 2 mg/mL, (C) 1 mg/mL, and (D) 0.5 mg/mL. CLSM analysis of biofilm formation in *C. violaceum* (CV12472), (E) untreated control strain of *C. violaceum* (CV12472), (F) in presence of EA extract at the concentration of 2 mg/mL, (G) 1 mg/mL, and (H) 0.5 mg/mL.

the structural complexities of the compounds. The EI/MS fragmentation patterns of individual compounds are presented in Figure S-1. The major chemical constituents of the EA extract were hexadecanoic acid (25.86%) at RT 13.975, 9,12-octadecenoic acid methyl ester at 15.824 with 18.77%, and *n*-octacosane at 21.297 with 12.0% as evident from the GC–MS spectra. Similarly, 9-octadecenoic acids (7.85%) at RT 16.071, hexadecanoic acid, 2-hydroxy-1-(hydroxymethyl) ethyl ester at 21.986 with 6.01% were identified with the minimum concentrations (Table 1 and Figure 4). The percentage of the remaining chemical constituents ranged from 4 to 0.6 and is represented in Table 1.

**2.4. Docking and Molecular Dynamics Analysis.** The CviR gene plays a significant role in QS, biofilm formation, and survival of *C. violaceum* (CV12472). A total of 20 different chemical compounds were identified by GC–MS, and the identified compounds were subjected to docking studies and also in predicting the binding score (Table 2 and Figure 5A–P). About the 20 compounds detected, hexadecanoic acid, 2-hydroxy-1-(hydroxymethyl) ethyl ester had a high affinity for the CviR receptor protein (Table 2), and hexadecanoic acid, 2-hydroxy-1-(hydroxymethyl) ethyl ester binds to the active site of CviR with a binding energy of  $-8.825$  kcal/mol, respectively (Table 2). The docked complex (CviR and compound) was subjected to MD simulations to check the stability and conformation changes of the CviR protein and hexadecanoic acid, 2-hydroxy-1-(hydroxymethyl) ethyl ester complex. The root-mean-square deviation (RMSD) (Figure 6A) and root-mean-square fluctuation (RMSF) values (Figure 6B) were observed up to 50 ns for CviR–hexadecanoic acid, 2-hydroxy-1-(hydroxymethyl) ethyl ester complexes, and the corresponding residues indicated the presence of glycine with radii of 1.77 and 2.73 Å (Gly-70) and hydrophobic contacts: Leu 72, Tyr 80, Leu 85, Tyr 88, Ile 99, Trp 111, Phe 115, and Phe 126. We also observed atomic exchange between protein, ligand, and complex systems throughout the simulation period. In addition, the major forces of the interaction in molecular association were hydrogen bonding, hydrophobic, and van der

Waals interactions. Figure 7A shows the 3D image representing the complex structure of CviR with hexadecanoic acid, 2-hydroxy-1-(hydroxymethyl) ethyl ester. Figure 7B,C shows the protein contact map and bar diagrams of the amino acids involved and their molecular properties, while superimposing and molecular dynamic simulations were performed.

### 3. DISCUSSION

We investigated the EA extract of *P. edulis* for their in vitro effects and in silico prediction of QS-controlled virulence factors and biofilm inhibitory activities against *C. violaceum* (CV12472). This is the first report to provide evidence that the EA extract of *P. edulis* possessed anti-QS and antibiofilm activities against *C. violaceum* (CV12472). The EA extract remarkably inhibited violacein pigment production in a dose-dependent manner (Figure 1A). The production of violacein pigment is regulated by the CviR-dependent QS system.<sup>43</sup> Others have shown that the methanolic extracts of the dried *Capparis spinosa* fruit inhibited violacein production up to 88% with a 2 mg/mL concentration.<sup>44</sup> Similarly, another report demonstrated that leaves of *Psidium guajava* (guava) inhibited the production of violacein by *C. violaceum*.<sup>45</sup>

Our study showed that the EA extract inactivated the production of AHL molecules at 72.5, 52.2, and 35.9%, which means that the EA extract interfered with QS by inhibiting the production of AHLs. One previous study revealed that a *trans*-cinnamaldehyde fraction interfered with the AHL-based QS system of *P. aeruginosa*.<sup>46</sup>

The EA extract also exhibited a drastic reduction in the swarming motility at various concentrations, viz., 2, 1, and 0.5 mg/mL, respectively, suggesting that the extract mitigated QS-dependent virulence factors and biofilm formation in *C. violaceum* (CV12472). The present data is in agreement with the findings of Abraham et al.<sup>44</sup> who reported that *C. spinosa* reduced the migration of *C. violaceum* (CV12472) swarming motility at a concentration of 100  $\mu$ g/mL. Similarly, leaf extracts of *Mangifera indica* (mango) significantly reduced swarming motility in *P. aeruginosa* in a dose-dependent



**Table 1. Compounds in EA Extract of *P. edulis* with Retention Time and Area (%). The Peak Numbers Match the Spectrum in Figure 4**

S.NO	Name of the bioactive compounds	Structure of the bioactive compounds	Molecular formula	Retention Time	Percentage %
1.	1-Hexadecene		C <sub>16</sub> H <sub>32</sub>	9.741	0.61
2.	9-Octadecene		C <sub>18</sub> H <sub>36</sub>	12.087	0.98
3.	Hexadecanoic acid, methyl ester		C <sub>17</sub> H <sub>34</sub> O <sub>2</sub>	13.560	2.77
4.	3-Tert-butyl-5-hydroxymethyl-cyclohex-2-enyl)-methanol		C <sub>13</sub> H <sub>22</sub> O <sub>2</sub>	13.774	0.75
5.	Hexadecanoic acid		C <sub>16</sub> H <sub>32</sub> O <sub>2</sub>	13.975	25.86
6.	9-Eicosane		C <sub>20</sub> H <sub>40</sub>	14.233	2.10
7.	n-Hexadecane		C <sub>16</sub> H <sub>34</sub>	14.292	0.63
8.	2-Hexadecanol		C <sub>16</sub> H <sub>34</sub> O	14.432	1.66
9.	9,12-Octadecadienoic acid methyl ester		C <sub>19</sub> H <sub>34</sub> O <sub>2</sub>	15.350	4.48
10.	8,11,14-Docosatrienoic acid methyl ester		C <sub>23</sub> H <sub>40</sub> O <sub>2</sub>	15.439	0.97
11.	9,12-Octadecenoic acid methyl ester		C <sub>19</sub> H <sub>34</sub> O <sub>2</sub>	15.824	18.77
12.	9-Octadecenoic acid		C <sub>18</sub> H <sub>34</sub> O <sub>2</sub>	16.071	7.85
13.	Cyclododecane		C <sub>12</sub> H <sub>24</sub>	16.343	2.48
14.	Dodecane, 2,7, 10-trimethyl-		C <sub>15</sub> H <sub>32</sub>	16.400	0.78
15.	n-Octacosane		C <sub>28</sub> H <sub>58</sub>	17.704	4.94
16.	n-Tricosane		C <sub>23</sub> H <sub>48</sub>	19.299	2.64
17.	9-Tricosene		C <sub>23</sub> H <sub>46</sub>	20.975	0.97
18.	n-Octacosane		C <sub>28</sub> H <sub>58</sub>	21.297	12.00
19.	Hexadecanoic acid, 2-hydroxy-1-(hydroxymethyl) ethyl ester		C <sub>19</sub> H <sub>38</sub> O <sub>4</sub>	21.986	6.01
20.	Heptadecane, 2,6,10,15-tetramethyl-		C <sub>21</sub> H <sub>44</sub>	23.833	2.75

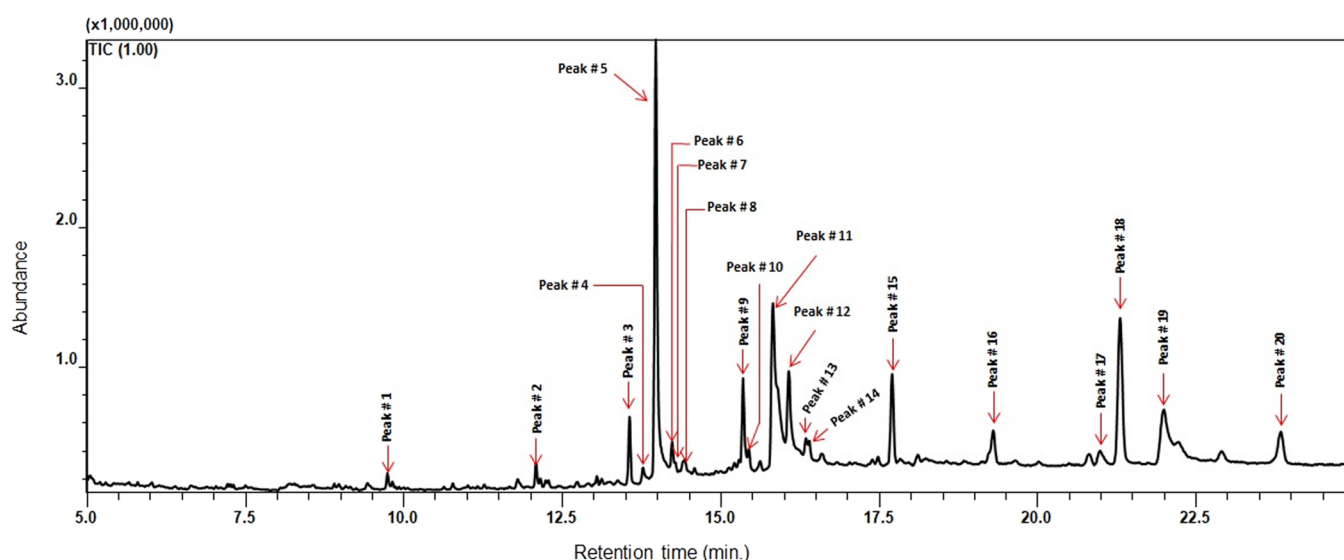


**Figure 4.** GC–MS chromatogram of *P. edulis* extract dissolved in *n*-hexane. The spectra of unknowns match well with spectra of WILEY7 library chromatogram, matching with compounds listed in Table 1.

**Table 2.** Predicted Docking Score Indicating the Binding Affinity Measured in Kilocalorie per Mole (kcal/mol) (CviR with Bioactive Compounds (Ligands) from EA Extract of *P. edulis* Fruits)

S. no	PubChem ID	bioactive compounds (ligands)	docking score (kcal/mol)	glide ligand efficiency	glide ligand efficiency sa	glide ligand efficiency ln	XP GScore	glide gscore
1	123,409	hexadecanoic acid, 2-hydroxy-1-hydroxymethyl ethyl ester	−8.825	−0.384	−1.091	−2.134	−8.825	−8.825
2	5,364,473	8,11,14-docosatrienoic acid methyl ester	−8.02	−0.321	−0.938	−1.901	−8.02	−8.02
3	6,385,060	9-tricosene	−7.945	−0.345	−0.982	−1.921	−7.945	−7.945
4	12,534	<i>n</i> -tricosane	−6.941	−0.302	−0.858	−1.678	−6.941	−6.941
5	41,209	heptadecane, 2,6,10,15-tetramethyl−	−6.351	−0.302	−0.834	−1.57	−6.351	−6.351
6	9268	cyclododecane	−6.312	−0.526	−1.204	−1.811	−6.312	−6.312
7	445,639	9-octadecenoic acid	−6.059	−0.303	−0.822	−1.516	−6.062	−6.062
8	5,282,457	9,12-octadecadienoic acid methyl ester	−5.98	−0.299	−0.812	−1.497	−5.984	−5.984
9	93,447	dodecane, 2,7,10-trimethyl−	−5.764	−0.384	−0.948	−1.555	−5.764	−5.764
10	5,364,599	9-octadecene	−5.522	−0.307	−0.804	−1.419	−5.522	−5.522
11	85,779	2-hexadecanol	−5.364	−0.316	−0.811	−1.399	−5.364	−5.364
12	8222	9-eicosane	−5.144	−0.257	−0.698	−1.287	−5.144	−5.144
13	985	hexadecanoic acid	−4.905	−0.273	−0.714	−1.261	−4.909	−4.909
14	8181	hexadecanoic acid methyl ester	−4.858	−0.256	−0.682	−1.232	−4.858	−4.858
15	12,395	1-hexadecene	−4.494	−0.281	−0.708	−1.191	−4.494	−4.494
16	11,006	<i>n</i> -hexadecane	−4.439	−0.277	−0.699	−1.177	−4.439	−4.439

manner.<sup>47</sup> EPS is one of the major virulence factors, which helps in maintaining the architecture of biofilm, microcolony formation, and prevents the entry of antimicrobial agents into a bacterial cell. Here, we showed that the EA extract of *P. edulis*, at sub-inhibitory concentrations (2, 1, and 0.5 mg/mL), decreased the production of EPS after 24 h of treatment. Thus, the EA extract has impeded the production of EPS and weakened biofilm formation in *C. violaceum* (CV12472). Champalal et al.<sup>48</sup> have reported that the amino acid lysine at a concentration of 0.684 mM, 14%, decreased the production of EPS in *C. violaceum* (CV12472).

The QS system is known to coordinate and regulate the biofilm architecture in a wide array of Gram-negative bacterial pathogens implicated with human infections. It plays a crucial role in the initiation, attachment, and maturation of sessile biofilms and also in disease pathogenesis and drug resistance. Therefore, an interference with the QS system may prevent the assembly of the biofilm matrix and the further establishment of

infection in host cells. The staining of the biofilm cell with crystal violet corroborated the effect of the EA extract of *P. edulis* on biofilm formation in *C. violaceum* (CV12472). This finding revealed that the EA extract can suppress the biofilm cluster significantly in a concentration-dependent manner without disturbing the planktonic cell growth (as depicted in Figure 1D). The obtained results are comparable with earlier reports.<sup>32,34,44</sup> In situ visualization indicated that the EA extract markedly reduced the biomass of the biofilm and also minimized microcolony formation, which were clearly evident from CLSM images. For further confirmation by light microscopy, this showed disintegrated architectures of the biofilm at the sub-MIC concentrations of 2, 1, and 0.5 mg/mL.

The GC–MS results were in accordance with Zahid et al.<sup>49</sup> who reported that the ethanolic and hexane fractions of *A. squamosa* seed chemical compounds (*n*-hexadecanoic acid, 9,12-octadecenoic acid methyl ester, *n*-octacosane, 9-octadecenoic acid, and hexadecanoic acid, 2-hydroxy-1-(hydroxy-



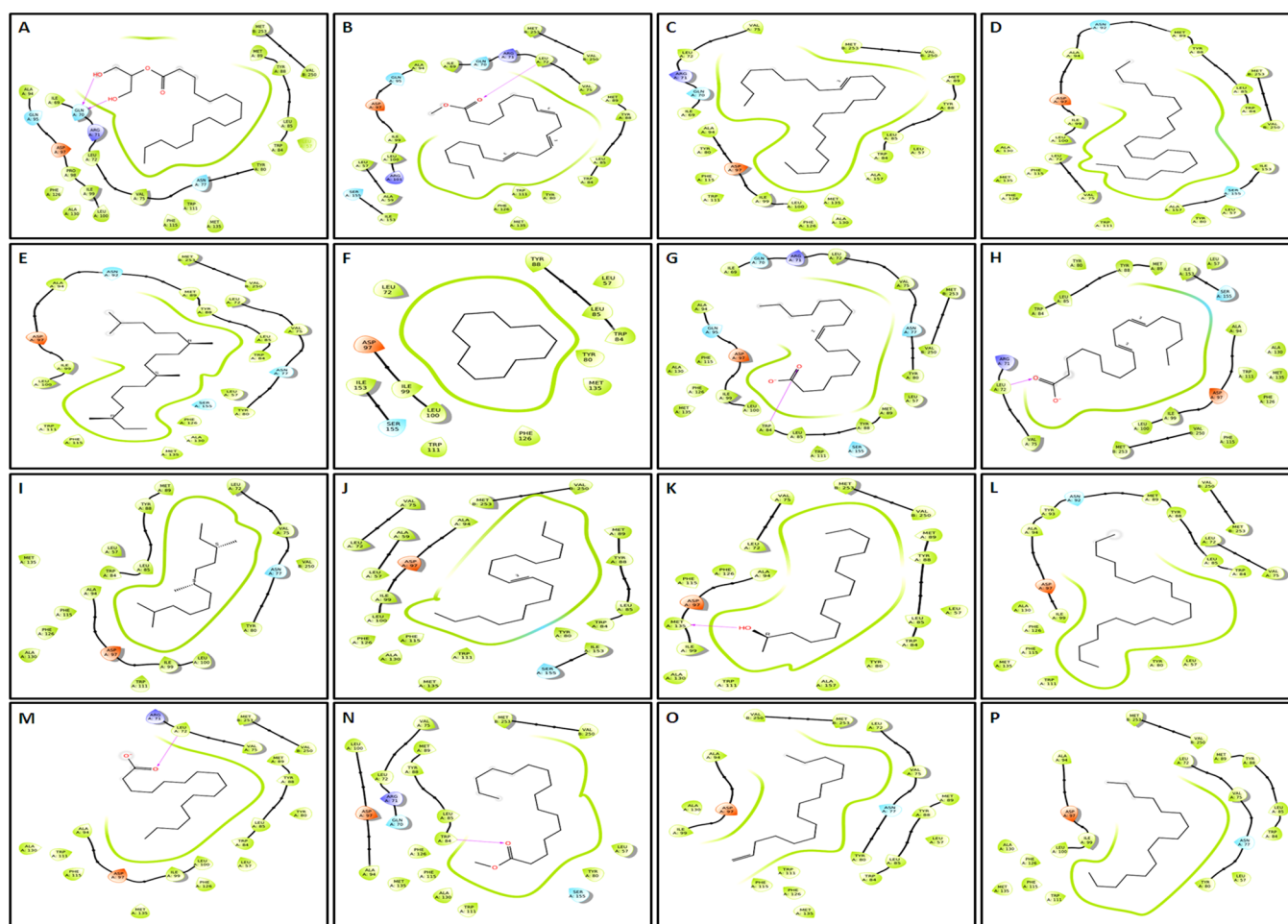


**Figure 5.** Schematic 2D interaction diagram representing the bonding between bioactive compounds (ligands) and the CviR (receptor) active site. The hydrogen bond formation is identified by blue line and hydrophobic contacts in yellow color. (A) Binding affinity of hexadecanoic acid, 2-hydroxy-1-(hydroxymethyl) ethyl ester–CviR, (B) 8,11,14-docosatrienoic acid methyl ester–CviR, (C) 9-tricosene–CviR, (D) *n*-tricosane–CviR, (E) heptadecane, 2,6,10,15-tetramethyl–CviR, (F) cyclododecane–CviR, (G) 9-octadecenoic acid–CviR, (H) 9,12-octadecadienoic acid methyl ester–CviR, (I) dodecane, 2,7,10-trimethyl–CviR, (J) 9-octadecene–CviR, (K) 2-hexadecanol–CviR, (L) 9-eicosane–CviR, (M) hexadecanoic acid–CviR, (N) hexadecanoic acid methyl ester–CviR, (O) 1-hexadecene–CviR, and (P) *n*-hexadecene–CviR complexes.

methyl) ethyl ester) were identified by GC–MS. Based on the GC–MS total ion chromatogram results (Figure S-1) and further, the identified bioactive compounds, via the docking and molecular dynamics, could contribute to improved the understanding of their mechanism of action. We have also successfully investigated the inhibitory activity and predicted binding scores by molecular docking and dynamics studies of *P. edulis* bioactive compounds (Figure 5A–P). Our identification of hexadecanoic acid, 2-hydroxy-1-(hydroxymethyl) ethyl ester interacting with the active site of CviR with the binding energy of  $-8.825$  kcal/mol has been reported by others.<sup>30</sup> Hydrogen bonding is the major contributor in the hot-spot identification. In this study, Gly 70 interacting through hydrogen bonding is significant in inducing QS activity in the CviR protein. Post docking, the CviR protein–hexadecanoic acid, 2-hydroxy-1-(hydroxymethyl) ethyl ester complex file was subjected to dynamic studies, which revealed that a conformation change likely has occurred in the protein. Consequently, fluctuated areas represented as RMSD and RMSF plots. 3D-imaging analysis also revealed the interaction between hexadecanoic acid, 2-hydroxy-1-(hydroxymethyl) ethyl ester and the CviR complex. Together, we concluded that hexadecanoic acid and 2-hydroxy-1-(hydroxymethyl) ethyl

ester could likely play a crucial role in suppressing the QS system in *C. violaceum* (CV12472).

## 4. CONCLUSIONS

The chemical constituents isolated and identified from the EA extract of *P. edulis*, and its active compounds appear to be potential candidates for investigating into their antipathogenic effects. It can probably serve to interfere with the AHL-based QS-controlled virulence factors and biofilm formation in *C. violaceum* (CV12472). The docking score and molecular dynamic studies have clearly suggested that hexadecanoic acid, 2-hydroxy-1-(hydroxymethyl) ethyl ester binds to the CviR receptor suggesting that the compound could be potentially used for treating *C. violaceum* infections. The anti-QS and antibiofilm abilities of the identified compounds need to be investigated in future studies for potential pharmacological and real-time therapeutic applications.

## 5. METHODS

**5.1. Bacterial Strain and Culture Conditions.** Wild-type *C. violaceum* (CV12472) isolates were routinely grown in sterile Luria Bertani (LB) (HiMedia, India) broth and

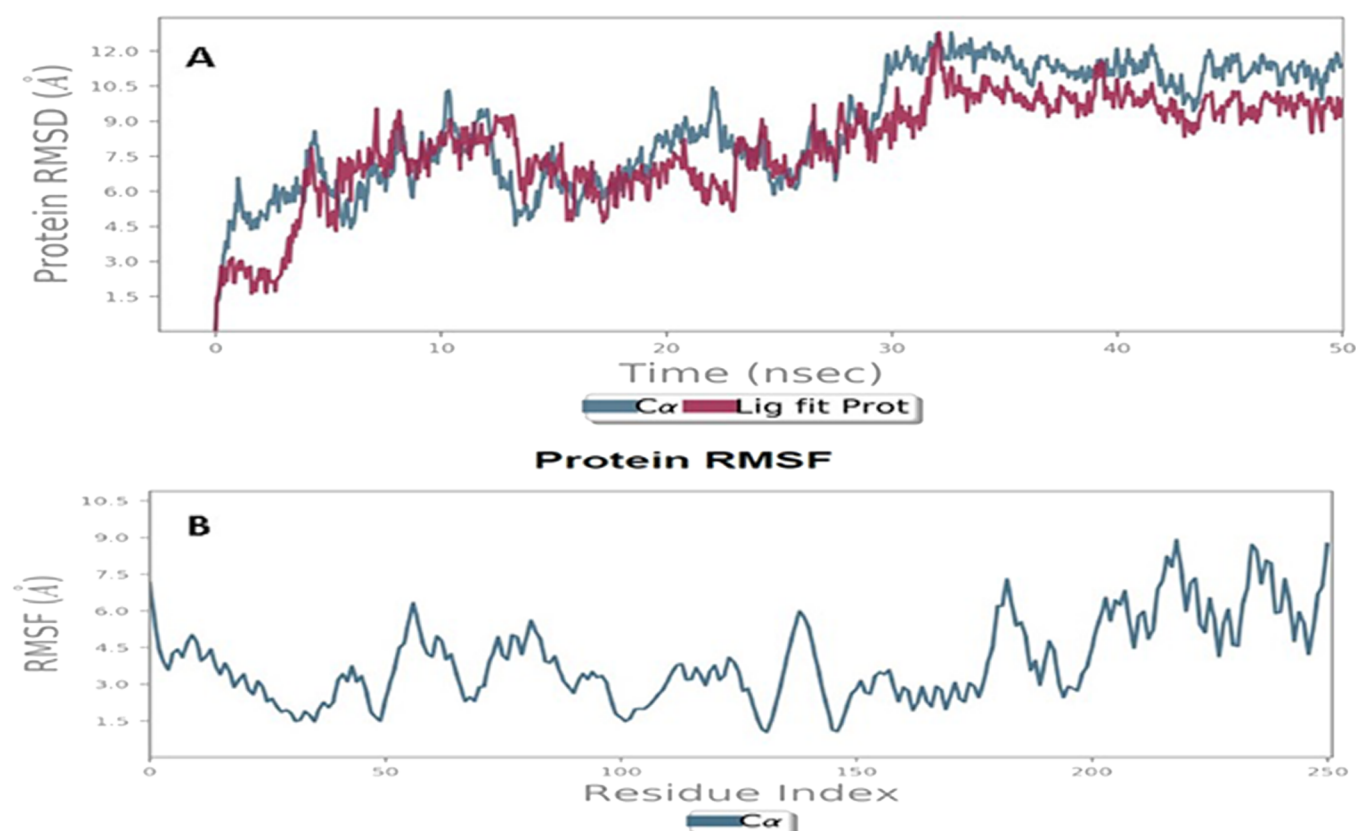


**Figure 6.** (A) RMSD and (B) RMSF plots showing the CviR protein backbone (Å) with the ligand interaction along residue numbers (50 ns). Fluctuated region identified has been shown in the XY scatter plot, especially 50–100 in residue index.

maintained at 30 °C with a shaker incubator (120 rpm) for 24 h.

## 5.2. Plant Product (Fruit) and Preparation of Extract.

Fruits of *P. edulis* were collected locally from Hubbathala (11.349°N, 76.759°E), Mettupalayam, Nilgiri District of Tamilnadu in southern India. The fruits were collected in sterile polyethylene bags and brought to the laboratory. The fleshy inner parts of *P. edulis* were taken in two separate screw-capped containers: one mixed with 100 mL of methanol and the other with 100 mL of ethyl acetate (EA). The extracts were constantly agitated in a shaker (120 rpm) for 3 days at room temperature. Subsequently, the methanol and EA extracts were filtered using a Whatman number 1 filter paper. The methanol and EA extracts were dried at 50 and 45 °C, respectively, using a rotary flash evaporator. The fruit extracts were further dried by vacuum concentration, and the residues were stored at 4 °C until further investigations.

**5.3. Evaluation of the Minimum Inhibitory Concentration of Crude Extracts.** The broth microdilution (two-fold) method was used to determine the minimum inhibitory concentrations (MICs) of methanol and EA fruit extracts of *P. edulis*. MICs of the methanol and EA fruit extracts against *C. violaceum* (CV12472) used in the assay were assessed in different concentrations ranging from 10 to 0.01 mg/mL. The growth of the bacteria was visualized by adding 2,3,5-triphenyl tetrazolium chloride (TTC) salt that acts as an indicator. The lowest concentration with no visible growth was recorded as MIC.<sup>31,32</sup>

**5.4. Quantification of Violacein.** The quantitative analysis of EA fruit (*P. edulis*) extracts on QS-controlled violacein production in *C. violaceum* (CV12472) was

determined by spectrophotometry as per protocols published by others.<sup>33,34</sup> Briefly, an 18 h ( $1 \times 10^8$  CFU/mL) old bacterial culture of *C. violaceum* (CV12472) was suspended in LB broth with both absence and presence of the EA fruit extract (*P. edulis*) and incubated at 30 °C for 24 h. Later, the bacterial cell pellets were dissolved in 200  $\mu$ L of DMSO. All the tubes were vortexed vigorously for the extraction of the violacein pigment. The bacterial cell debris was removed by centrifugation, and absorbance of soluble violacein was read at 585 nm (Thermo Scientific, Mumbai, India) using a microtitre plate reader (Nest Biotech Co., Ltd., China). The percentage of growth of the treated *C. violaceum* (CV12472) strain was compared with the untreated control by measuring the OD at 600 nm. The percentage of violacein pigment in the presence of EA fruit extracts was calculated by eq 1

$$\begin{aligned} &\% \text{violacein inhibition} \\ &= \left( \frac{\text{assay control OD at 585 nm} - \text{unknown sample OD at 585 nm}}{\text{assay control OD at 585}} \right) \\ &\times 100 \end{aligned} \quad (1)$$

**5.5. Quantification of Acyl Homoserine Lactones (AHLs).** HSL extraction (liquid–liquid extraction) was described by spectrophotometry as per protocols published by others.<sup>35</sup> Briefly, 20  $\mu$ L of *C. violaceum* CV12472 was suspended in [with (2, 1, and 0.5 mg/mL) or without EA fruit extract] 180  $\mu$ L of LB medium and the tubes were incubated at 30 °C for 24 h in a shaker incubator. Later, the cell supernatants were transferred into fresh test tubes. The equal volume of acidified ethyl acetate (0.5%, glacial acetic acid) was added, and the tubes were mixed well. The organic layer of both treated and control tubes were separated. The organic



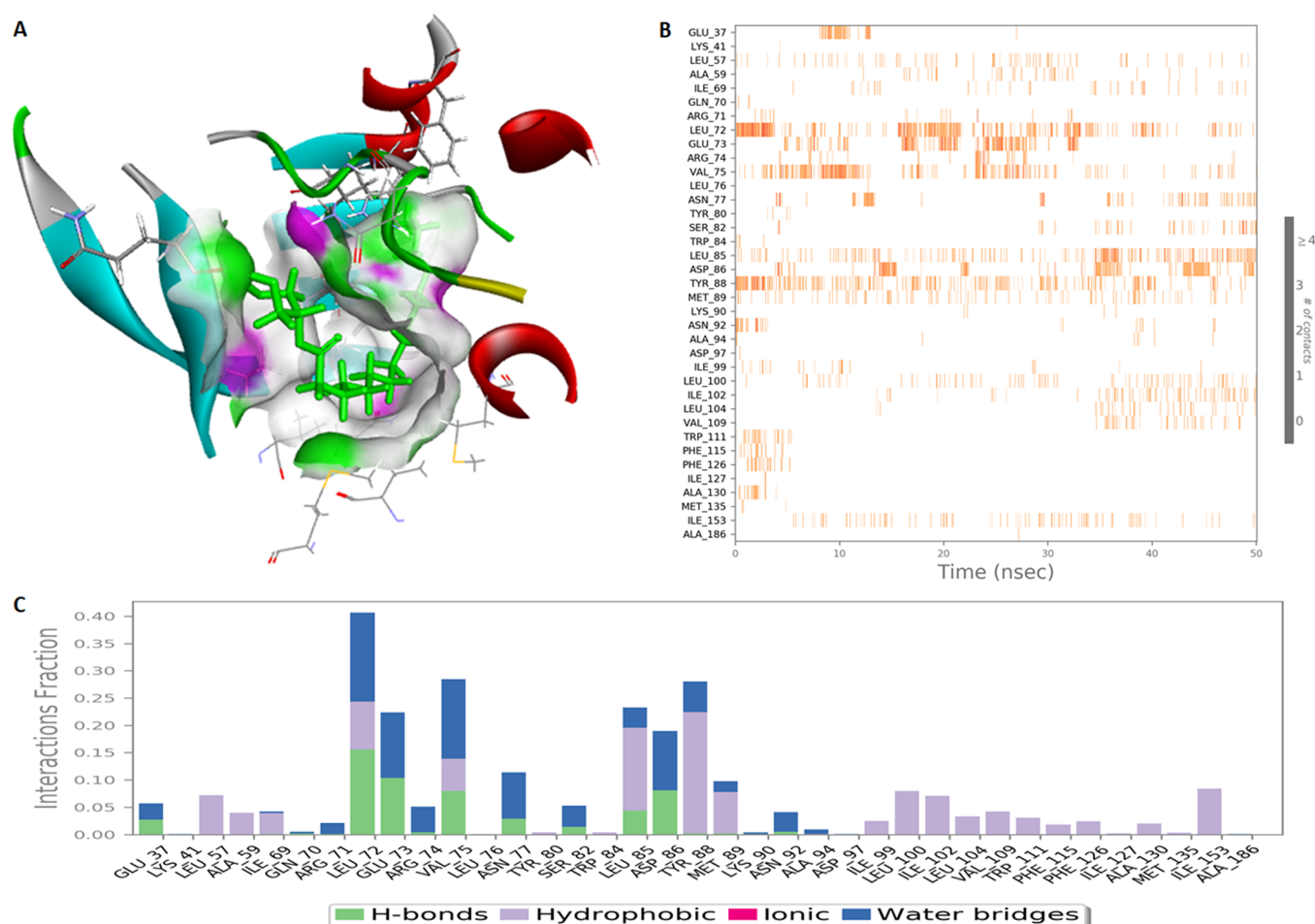


**Figure 7.** (A) Schematic 3D image shows the interactions between hexadecanoic acid, 2-hydroxy-1-hydroxymethyl ethyl ester, and CviR complex; (B) during the trajectory preparation, first 5 ns, the poses were increased (orange color shades) in simulation, i.e., Leu 72, Val 75, and Tyr 88, respectively; (C) histogram of the protein–ligand contact map: CviR–hexadecanoic acid, 2-hydroxy-1-hydroxymethyl ethyl ester complex.

layer was distilled and dried using the rotary flash evaporator at 45 °C. The residues were resuspended in 20% acidified ethyl acetate and stored at −20 °C for further use. To each of the wells, residues (both control and treated) were loaded and equal volume of the mixture (hydroxyl amine (2 M)/NaOH (3.5 M), 1:1 ratio) were loaded. Subsequently, equal volumes of a mixture of ferric chloride (4 M HCl (10%)) and 95% ethanol were added, and OD was set at 520 nm.

**5.6. Swarming Motility.** Swarming motility was performed using the method described elsewhere.<sup>32</sup> Briefly, the LB medium (1% (w/v) tryptone, 0.5% (w/v) NaCl, 0.2% (w/v) glucose, and 0.5% (w/v) agar) supplemented with or without the EA fruit extract at different concentrations (2, 1, and 0.5 mg/mL) were point-inoculated with the overnight culture of *C. violaceum* (CV12472). The plates were incubated at 30 °C for 18 h. After incubation, both treated and untreated plates were observed for measuring the diameters of the motility zone.

**5.7. Extraction and Quantification of Exopolysaccharide (EPS).** Extraction of EPS was performed using the method described elsewhere.<sup>32</sup> Briefly, 20  $\mu$ L of the overnight culture of *C. violaceum* (CV12472) and EA fruit extracts were loaded in a dose-dependent manner (2, 1, and 0.5 mg/mL) into 180  $\mu$ L of LB medium and without the extract as a control. All the tubes were incubated at 30 °C for 24 h. The bacterial cell pellets were resuspended in high-salt buffer and

centrifuged at 10,000 rpm. An equal volume of ethanol was added to the collected supernatant and centrifuged at 10,000 rpm for 30 min. The precipitated EPS (1 mL) was mixed with 1 mL of cold 5% phenol and 5 mL of concentrated H<sub>2</sub>SO<sub>4</sub> until a red color developed, and the intensity of the color was measured at 490 nm using a spectrophotometer.

**5.8. Biofilm Inhibition Assay.** The effect of EA extracts on biofilm formation by *C. violaceum* (CV12472) was determined by the crystal violet staining assay.<sup>32–36</sup> Briefly, 20  $\mu$ L of overnight growth of *C. violaceum* (CV12472) and EA fruit extracts were loaded in a dose-dependent manner (2, 1, and 0.5 mg/mL) into 180  $\mu$ L of the LB medium (supplemented with 0.2% (w/v) glucose) and incubated at 30 °C for 24 h. The planktonic cells were removed by washing with sterile water, and the surface-adherent biofilm was stained with a 0.1% crystal violet solution. After 15 min, the unbound crystal violet was washed with sterile-distilled water. Finally, the adherent biofilm-bound crystal violet was eluted in 200  $\mu$ L of ethanol (95%) and quantified by measuring the intensity of crystal violet at 585 nm using a UV–vis spectrophotometer.

**5.9. In Situ Visualization of the *C. violaceum* Biofilm.** The light microscopic analysis method described for biofilm formation on a glass cover slip was performed as described previously.<sup>37</sup> Briefly, the *C. violaceum* (CV12472) isolate was added to the fresh LB medium (supplemented with 0.2% (w/v) glucose) containing glass cover slips using a 6-well flat

bottom microtitre plate with EA fruit extracts and along with appropriate control wells without the extracts. The plate was incubated in a static condition at 30 °C for 24 h. After incubation, the unbound planktonic cells from both treated and untreated glass cover slips were removed, rinsed with sterile distilled water, and stained with 0.2% crystal violet. Excessive crystal violet was washed twice with sterile-distilled water, and the stained-glass cover slips together with the adherent biofilm were visualized under a light microscope (Olympus, CX23, China).

For confocal laser electron microscopy analysis, the adherent biofilms of both treated and untreated glass cover slips were washed twice with distilled water and stained with 0.1% acridine orange. Later, the biofilms were visualized using a confocal laser scanning microscope (CLSM) (Leica, TCS SP8, India).

**5.10. Gas Chromatography–Mass Spectrum (GC–MS) Analysis.** GC–MS analysis was performed as described previously.<sup>32</sup> Briefly, the EA fruit extract was analyzed by a Shimadzu GCMSQP-2010 plus detector gas chromatograph equipped with a RTx-5MS (30.0 m × 0.32 mm ID., 0.5 μm thickness) crossbond diphenyl dimethyl polysiloxane-fused silica capillary column. Helium, ≥99.99%, was used as a carrier gas with a constant flow rate of 0.8 mL/min. The previously concentrated EA fruit extract was dissolved in *n*-hexane, and 1 μL of the sample was injected (split ratio of 100:1) into GC–MS using an AOC5000 auto-injector. The GC–MS chromatogram obtained was matched by NIST/WILEY7 library database.

**5.11. Molecular Docking Studies of CviR and Natural Compounds.** Molecular docking studies were carried out using Schrodinger maestro software, version 9.2. The binding affinities of the identified EA fruit chemical compounds from GC–MS analysis and the natural autoinducer to the transcriptional receptor, CviR protein (PDB ID: 3QP5), were retrieved from PubChem and protein Data Bank.<sup>38</sup> In the crystal structure, missing residues were added and water molecules around the receptor were removed using protein preparation wizard. The crystal structure, active site, and grid generation were adjusted with cocrystallized compounds. The chemical compound energy minimizing, rotatable bonds, and hydrogen bond optimization were executed with an OPLS force field. The interaction of the receptor and ligands prepared using maestro, Schrodinger suite. Docking of all the compounds with receptor was consequently performed using the glide<sup>39</sup> module to analyze the conformations of the protein–ligand complex using molecular dynamic methods.<sup>40</sup> Molecular dynamics and simulations were calculated up to 50 ns by the Desmond module<sup>41</sup> as evident to the movement of atoms. The protein–ligand complex was set into the orthorhombic box with a simple point charge water model, and charges were neutralized by adding sodium and chloride ions in the simulation. Steric clashes were executed to adhere with conformation change, and subsequently, the charges were minimized. A complex system was adjusted to the temperature of 300 K and 1 bar pressure in terms of NVT and NPT ensemble analyses. In addition to simulation, the root-mean-square deviation (RMSD), root-mean-square fluctuation (RMSF), radius of gyration (rGyr), solvent-accessible surface area (SASA), secondary structure elements (SSE), and torsional profile were recorded along with the  $\alpha$ -carbon backbone.<sup>42</sup>

**5.12. Statistical Analysis.** All in vitro experiments were performed in triplicates, and statistical significance for the quantification of violacein pigment, AHLs, EPS, and biofilm was determined by one-way ANOVA followed by Tukey's test ( $P < 0.05$ ) using GraphPad Prism 5.03 software (Graph Pad Software Inc., La Jolla, CA, USA).

## ■ ASSOCIATED CONTENT

### ● Supporting Information

The Supporting Information is available free of charge at <https://pubs.acs.org/doi/10.1021/acsomega.0c02483>.

Electrospray ion chromatogram and mass spectrum of EA extract of *P. edulis* bioactive compounds as analyzed by GC–MS (PDF)

## ■ AUTHOR INFORMATION

### Corresponding Authors

**Jamuna Vadivelu** — Department of Medical Microbiology, Faculty of Medicine, University of Malaya, Lembah Pantai, Kuala Lumpur 50603, Malaysia; Email: [jamuna@um.edu.my](mailto:jamuna@um.edu.my)  
**Esaki Muthu Shankar** — Infection Biology, Department of Life Sciences, Central University of Tamil Nadu, Thiruvavur 610 005, India; [orcid.org/0000-0002-7866-9818](https://orcid.org/0000-0002-7866-9818); Email: [shankarem@cutn.ac.in](mailto:shankarem@cutn.ac.in)

### Authors

**Mahendrarajan Venkatramanan** — Infection Biology, Department of Life Sciences, Central University of Tamil Nadu, Thiruvavur 610 005, India  
**Pitchaipillai Sankar Ganesh** — Infection Biology, Department of Life Sciences, Central University of Tamil Nadu, Thiruvavur 610 005, India  
**Renganathan Senthil** — Department of Bioinformatics, Marudupandiyar College, Thanjavur 613403, India; Lysine Biotech Private Limited, Periyar Maniammai University, Thanjavur 613403, India  
**Jeyachandran Akshay** — Infection Biology, Department of Life Sciences, Central University of Tamil Nadu, Thiruvavur 610 005, India  
**Arumugam Veera Ravi** — Department of Biotechnology, Alagappa University, Karaikudi 630 003, India  
**Kulanthaiivel Langeswaran** — Department of Bioinformatics, Alagappa University, Karaikudi 630 003, India  
**Samuthira Nagarajan** — Department of Chemistry, Central University of Tamil Nadu, Thiruvavur 610 005, India; [orcid.org/0000-0001-6959-7747](https://orcid.org/0000-0001-6959-7747)  
**Kaliaperumal Rajendran** — Department of Chemistry, Cape Breton University, Sydney, Nova Scotia B1P 6L2, Canada

Complete contact information is available at: <https://pubs.acs.org/doi/10.1021/acsomega.0c02483>

### Author Contributions

♦M.V. and P.S.G. equally contributed to this work and should therefore be considered as co-first authors. P.S.G. and E.M.S. designed the study. M.V. and P.S.G. performed the in vitro study. M.V. performed the in situ experiments. P.S.G., S.N., and K.R. analyzed and interpreted the GC–MS data. R.S. and P.S.G. performed the docking and molecular dynamics studies. E.M.S. provided funding support for the current work. P.S.G., J.V., and E.M.S. wrote the manuscript. M.V., P.S.G., R.S., J.A., V.R.A., K.L., J.V., S.N., K.R., and E.M.S. approved the final version of the manuscript.



## Notes

The authors declare no competing financial interest.

## ■ ACKNOWLEDGMENTS

The authors are thankful to Dr. S. Usha, Integrating Biocomputing Lab, Department of Bioinformatics, Bharathiar University, Coimbatore, for providing the computing facilities. The authors also thank Prof. Kavitha Louis, Mr. Yesu Raja, Mr. Charan Prasad (Department of Physics), Ms. Devi Bala (Department of Chemistry), Dr. Dinakar Challabathula, Mr. Benedict Analin, Ms. Zarin Taj, Mr. Akhil Mohanan (Plant Stress Physiology Group), Mr. Nehru Raja, and Ms. Latha (Department of Life Sciences), Central University of Tamil Nadu, Thiruvavur, for thoughtful and constructive discussions. The work was partially supported by Frontiers Research Grant (No FG012-17AFR), University of Malaya, Kuala Lumpur, Malaysia, for Prof. Jamuna Vaideluvu. The authors gratefully acknowledge Ms. Jaisheela Vimali and Ms. S. Vishnupriya, Infection Biology, Department of Life Sciences, Central University of Tamil Nadu, Thiruvavur, for generously providing fruits of *Passiflora edulis* collected from Mettupalayam as a gift for the research work.

## ■ ABBREVIATIONS

AHL, acyl-homoserine lactone; AIs, auto inducers; CFU, colony forming unit; C10-HSL, *N*-decanoyl-L-homoserine lactone; CLSM, confocal laser scanning microscope; EA, ethyl acetate; EI-MS, electron impact–mass spectra; EPS, exopolysaccharide; GC–MS, gas chromatography and mass spectroscope; LB, luria bertani; MIC, minimum inhibitory concentration; NPT, constant number pressure temperature; NVT, constant number volume temperature; QS, quorum sensing; RMSD, root-mean-square deviation; RMSF, root-mean-square fluctuations; RT, retention time; SASA, solvent-accessible surface area; SSE, secondary structure elements; TIC, total ion chromatogram; TTC, 2,3,5-triphenyl tetrazolium chloride; W/V, weight/volume.

## ■ REFERENCES

(1) Howard, A. J.; Ison, C. A. *Haemophilus, Gardnerella and other bacilli*; Collee, J. G., Fraser, A. G., Marmion, B. P., Simmons, A. Eds.; 14th ed, Mackie and McCartney Practical Medical Microbiology: New York, 1996. pp. 329–41.

(2) Sharmin, S.; Jahan, A. A.; Kamal, S. M. M.; Sarker, P. Fatal Infection Caused by *Chromobacterium violaceum*: A case report from a tertiary care hospital in Bangladesh. *Case Rep. Infect. Dis.* **2019**, 1.

(3) Slesak, G.; Douangdala, P.; Inthalad, S.; Silisouk, J.; Vongsouvath, H.; Sengduangphachanh, A.; Moore, C. E.; Mayxay, M.; Matsuoka, H.; Newton, P. N. Fatal *Chromobacterium violaceum* septicaemia in northern Laos, a modified oxidase test and post-mortem forensic family G6PD analysis. *Ann. Clin. Microbiol. Antimicrob.* **2009**, 8, 24.

(4) Kumar, M. R. *Chromobacterium violaceum*: A rare bacterium isolated from a wound over the scalp. *Int. J. Appl. Basic Med. Res.* **2012**, 2, 70–72.

(5) Hagiya, H.; Murase, T.; Suzuki, M.; Shibayama, K.; Kokumai, Y.; Watanabe, N.; Maki, M.; Otsuka, F. *Chromobacterium violaceum* nosocomial pneumonia in two Japanese patients at an intensive care unit. *J. Infect. Chemother.* **2014**, 20, 139–142.

(6) Pant, N. D.; Acharya, S. P.; Bhandari, R.; Yadav, U. N.; Saru, D. B.; Sharma, M. Bacteremia and urinary tract infection caused by *Chromobacterium violaceum*: case reports from a tertiary care hospital in Kathmandu, Nepal. *Case Rep. Med.* **2017**, 2017, 1.

(7) Casalta, J. P.; Peloux, Y.; Raoult, D.; Brunet, P.; Gallais, H. Pneumonia and meningitis caused by a new nonfermentative

unknown gram-negative bacterium. *J. Clin. Microbiol.* **1989**, 27, 1446–1448.

(8) Kaniyarakkal, V.; Orvankundil, S.; Lalitha, S. K.; Thazhethkandi, R.; Thottathil, J. *Chromobacterium violaceum* septicaemia and urinary tract infection: Case reports from a tertiary care hospital in South India. *Case Rep. Infect. Dis.* **2016**, 2016, 1.

(9) Yang, C.-H.; Li, Y.-H. *Chromobacterium violaceum* infection: A clinical review of an important but neglected infection. *J. Chin. Med. Assoc.* **2011**, 74, 435–441.

(10) Høiby, N.; Bjørnsholt, T.; Givskov, M.; Molin, S.; Ciofu, O. Antibiotic resistance of bacterial biofilms. *Int. J. Antimicrob. Agents* **2010**, 35, 322–332.

(11) McClean, K. H.; Winson, M. K.; Fish, L.; Taylor, A.; Chhabra, S. R.; Camara, M.; Daykin, M.; Lamb, J. H.; Swift, S.; Bycroft, B. W.; Stewart, G. S. A. B.; Williams, P. Quorum sensing and *Chromobacterium violaceum*: expression of violacein production and inhibition for the detection of *N*-acyl homoserine lactones. *Microbiology* **1997**, 143, 3703–3711.

(12) Stauff, D. L.; Bassler, B. L. Quorum sensing in *Chromobacterium violaceum*: DNA recognition and gene regulation by the CviR receptor. *J. Bacteriol.* **2011**, 193, 3871–3878.

(13) Brumbach, K. C.; Eason, B. D.; Anderson, L. K. The *Serratia*-type hemolysin of *Chromobacterium violaceum*. *FEMS Microbiol. Lett.* **2007**, 267, 243–250.

(14) Ciprandi, A.; da Silva, W. M.; Santos, A. V.; de Castro Pimenta, A. M.; Carepo, M. S. P.; Schneider, M. P. C.; Azevedo, V.; Silva, A. *Chromobacterium violaceum*: Important insights for virulence and biotechnological potential by exoproteomics studies. *Curr. Microbiol.* **2013**, 67, 100–106.

(15) de Brito, C. F. A.; Carvalho, C. M. B.; Santos, F. R.; Gazzinelli, R. T.; Oliveira, S. C.; Azevedo, V.; Teixeira, S. M. R. *Chromobacterium violaceum* genome: molecular mechanisms associated with pathogenicity. *Genet. Mol. Res.* **2004**, 3, 148–161.

(16) Greenberg, E. P. Quorum sensing in gram negative bacteria. *ASM News* **1997**, 63, 371–377.

(17) Batista, J. H.; da Silva Neto, J. F. *Chromobacterium violaceum* pathogenicity: updates and insights from genome sequencing of novel *Chromobacterium* Species. *Front. Microbiol.* **2017**, 8, 2213.

(18) Aldridge, K. E.; Valainis, G. T.; Sanders, C. V. Comparison of the *in vitro* activity of ciprofloxacin and 24 other antimicrobial agents against clinical strain of *Chromobacterium violaceum*. *Diagn. Microbiol. Infect. Dis.* **1988**, 10, 31–39.

(19) Hall, C. W.; Mah, T.-F. Molecular mechanisms of biofilm-based antibiotic resistance and tolerance in pathogenic bacteria. *FEMS Microbiol. Rev.* **2017**, 41, 276–301.

(20) Barroso, K. C. M.; Previato-Mello, M.; Batista, B. B.; Batista, J. H.; da Silva Neto, J. F. EmrR-dependent upregulation of the efflux pump EmrCAB contributes to antibiotic resistance in *Chromobacterium violaceum*. *Front. Microbiol.* **2018**, 9, 2756.

(21) Ganesh, P. S.; Vishnupriya, S.; Vaideluvu, J.; Mariappan, V.; Vellamy, K. M.; Shankar, E. M. Intracellular survival and innate immune evasion of *Burkholderia cepacia*: Improved understanding of quorum sensing-controlled virulence factors, biofilm, and inhibitors. *Microbiol. Immunol.* **2020**, 64, 87–98.

(22) Pena, R. T.; Blasco, L.; Ambroa, A.; González-Pedrajo, B.; Fernández-García, L.; López, M.; Bleriot, I.; Bou, G.; García-Contreras, R.; Wood, T. K.; Tomás, M. Relationship between quorum sensing and secretion systems. *Front. Microbiol.* **2019**, 10, 1100.

(23) Sibanda, S.; Moleleki, L. N.; Shyntum, D. Y.; Coutinho, T. A. Quorum sensing in gram-negative plant pathogenic bacteria. *Adv. Plant. Pathol.* **2018**, DOI: 10.5772/intechopen.78003.

(24) Tshikalange, T. E.; Modishane, D. C.; Tabit, F. T. Antimicrobial antioxidant, and cytotoxicity properties of selected wild edible fruits of traditional medicinal plants. *J. Herbs, Species Med. Plants* **2017**, 23, 1–76.

(25) Rasmussen, T. B.; Bjørnsholt, T.; Skindersoe, M. E.; Hentzer, M.; Kristoffersen, P.; Köté, M.; Nielsen, J.; Eberl, L.; Givskov, M. Screening for quorum-sensing inhibitors (QSI) by use of a novel

genetic system, the QSI selector: a bargain of effects. *J. Bacteriol.* **2006**, *187*, 895–1814.

(26) Girennavar, B.; Cepeda, M. L.; Soni, K. A.; Vikram, A.; Jesudhasan, P.; Jayaprakasha, G. K.; Pillai, S. D.; Patil, B. S. Grape fruit juice and furocoumarins inhibits autoinducer signaling and biofilm formation in bacteria. *Int. J. Food Microbiol.* **2008**, *125*, 204–208.

(27) Vikram, A.; Jesudhasan, P. R.; Jayaprakasha, G. K.; Pillai, B. S.; Patil, B. S. Grapefruits bioactive limonoids modulate *E. coli* O157:H7 TTSS and antibiofilm. *Int. J. Food Microbiol.* **2010**, *140*, 109–116.

(28) Musthafa, K. S.; Ravi, A. V.; Annapoorani, A.; Packiavathy, I. S. V.; Pandian, S. K. Evaluation of anti-quorum-sensing activity of edible plants and fruits through inhibition of the N-acyl-homoserine lactone system in *Chromobacterium violaceum* and *Pseudomonas aeruginosa*. *Chemotherapy* **2010**, *56*, 333–339.

(29) Thokchom, R.; Mandal, G. Production preference and importance of passion fruit (*Passiflora edulis*): A review. *J. Agric. Eng. Food Technol.* **2017**, *4*, 27–30.

(30) Dhawan, K.; Dhawan, S.; Sharma, A. *Passiflora*: a review update. *J. Ethnopharmacol.* **2004**, *94*, 1–23.

(31) Packiavathy, I. A. S. V.; Agilandewari, P.; Musthafa, K. S.; Pandian, S. K.; Ravi, A. V. Antibiofilm and quorum sensing inhibitory potential of *Cuminum cyminum* and its secondary metabolite methyl eugenol against Gram negative bacterial pathogens. *Food Res. Int.* **2012**, *45*, 85–92.

(32) Ganesh, P. S.; Vittal, R. R. *In vitro* antibiofilm activity of *Murraya koenigii* essential oil extracted using supercritical fluid CO<sub>2</sub> method against *Pseudomonas aeruginosa* PAO1. *Nat. Prod. Res.* **2015**, *29*, 2295–2298.

(33) Blosser, R. S.; Gray, K. M. Extraction of violacein from *Chromobacterium violaceum* provides a new quantitative bioassay for N-acyl homoserine lactone autoinducers. *J. Microbiol. Methods* **2000**, *40*, 47–55.

(34) Ganesh, P. S.; Rai, V. R. Attenuation of quorum-sensing-dependent virulence factors and biofilm formation by medicinal plants against antibiotic resistant *Pseudomonas aeruginosa*. *J. Tradit. Complementary Med.* **2018**, *8*, 170–177.

(35) Taghadosi, R.; Shakibaie, M. R.; Masoumi, S. Biochemical detection of N-acyl homoserine lactone from biofilm-forming uropathogenic *Escherichia coli* isolated from urinary tract infection samples. *Rep. Biochem. Mol. Biol.* **2015**, *3*, 56–61.

(36) O'Toole, G. A.; Kolter, R. Initiation of biofilm formation in *Pseudomonas fluorescens* WCS365 proceeds via multiple convergent signaling pathways: a genetic analysis. *Mol. Microbiol.* **1998**, *28*, 449–461.

(37) Gopu, V.; Shetty, P. H. Cyanidin inhibits quorum signaling pathway of a food-borne opportunistic pathogen. *J. Food Sci. Technol.* **2016**, *53*, 968–976.

(38) Berman, H. M.; Battistuz, T.; Bhat, T. N.; Bluhm, W. F.; Bourne, P. E.; Burkhardt, E.; Feng, Z.; Gilliland, G. L.; Iype, L.; Jain, S.; Fagan, P.; Marvin, J.; Padilla, D.; Ravichandran, V.; Schneider, B.; Thanki, N.; Weissig, H.; Westbrook, J. D.; Zardecki, C. The protein data bank. *Acta Crystallogr., Sect. D: Struct. Biol.* **2002**, *58*, 99–907.

(39) Friesner, R. A.; Murphy, R. B.; Repasky, M. P.; Frye, L. L.; Greenwood, J. R.; Halgren, T. A.; Sanschagrin, P. C.; Mainz, D. T. Extra precision glide: Docking and scoring incorporating a model of hydrophobic enclosure for protein–ligand complexes. *J. Med. Chem.* **2006**, *49*, 6177–6196.

(40) Senthil, R.; Sakthivel, M.; Usha, S. Structure-based drug design of peroxisome proliferator activated receptor gamma inhibitors: Ferulic acid and derivatives. *J. Biomol. Struct. Dyn.* **2020**, 1–17.

(41) Shaw, D. E. *Desmond Molecular Dynamics System*; Schrödinger: New York, NY, 2014.

(42) Bucio-Cano, A.; Reyes-Arellano, A.; Correa-Basurto, J.; Bello, M.; Torres-Jaramillo, J.; Salgado-Zamora, H.; Curiel-Quesada, E.; Peralta-Cruz, J.; Avila-Sorrosa, A. Targeting quorum sensing by designing azoline derivatives to inhibit the N-hexanoyl homoserine lactone-receptor CviR: Synthesis as well as biological and theoretical evaluations. *Bioorg. Med. Chem.* **2015**, *23*, 7565–7577.

(43) McLean, R. J. C.; Pierson, L. S., III; Fuqua, C. A simple screening protocol for the identification of quorum signal antagonists. *J. Microbiol. Methods* **2004**, 351–360.

(44) Abraham, S. V. P. I.; Palani, A.; Ramaswamy, B. R.; Shunmugiah, K. P.; Arumugam, V. R. Anti-quorum sensing and antibiofilm potential of *Capparis spinosa*. *Arch. Med. Res.* **2011**, *42*, 658–668.

(45) Ghosh, R.; Tiwary, B. K.; Kumar, A.; Chakraborty, R. Guava leaf extract inhibits quorum-sensing and *Chromobacterium violaceum* induced lysis of human hepatoma cells: transcriptome analysis reveals differential gene expression. *PLoS One* **2014**, *9*, No. e107703.

(46) Chang, C.-Y.; Krishnan, T.; Wang, H.; Chen, Y.; Yin, W.-F.; Chong, Y. M.; Tan, L. Y.; Chong, T. M.; Chan, K.-G. Non-antibiotic quorum sensing inhibitors acting against N-acyl homoserine lactone synthase as druggable target. *Sci. Rep.* **2014**, *4*, 7245.

(47) Husain, F. M.; Ahmad, I.; Al-thubiani, A. S.; Abulreesh, H. H.; AlHazza, I. M.; Aqil, F. Leaf extract of *Mangifera indica* L. inhibit quorum sensing-regulated production of virulence factors and biofilm in test bacteria. *Front. Microbiol.* **2017**, *8*, 727.

(48) Champalal, L.; Kumar, U. S.; Krishnan, N.; Vaseeharan, B.; Mariappanadar, V.; Raman, P. Modulation of quorum sensing-controlled virulence factors in *Chromobacterium violaceum* by selective amino acids. *FEMS Microbiol. Lett.* **2018**, *3*, fny252.

(49) Zahid, M.; Arif, M.; Rahman, A.; Singh, K.; Mujahid, M. Solvent extraction and gas chromatography–mass spectrometry analysis of *Annona squamosa* L. seeds for determination of bioactives, fatty acid/fatty oil composition, and antioxidant activity. *J. Diet. Suppl.* **2017**, *15*, 613–623.

(50) Sun, S.; Dai, X.; Sun, J.; Bu, X.; Weng, C.; Li, H.; Zhu, H. A diketopiperazine factor from *Rheinheimera aquimaris* QSI02 exhibits anti-quorum sensing activity. *Sci. Rep.* **2016**, *6*, 39637.